Available online at www.sciencedirect.com
ScienceDirect
Journal of Photochemistry and Photobiology A: Chemistry 190 (2007) 283–289
Journal of Photochemistry and Photobiology A:Chemistry
www.elsevier.com/locate/jphotochem

Water effect on the excited-state decay paths of singlet excited cytosine

Lluís Blancafort *, Annapaola Migani

Institut de Química Computacional, Departament de Química, Universitat de Girona, Campus de Montilivi 17071, Spain

Available online 19 April 2007

Abstract

Two low-energy deactivation paths for singlet excited cytosine, one through a S_1/S_0 conical intersection of the ethylene type, and one through a conical intersection that involves the (n_N, π^*) state, are calculated in the presence of water. Water is included explicitly for several cytosine monohydrates, and as a bulk solvent, and the calculations are carried out at the complete active space self-consistent field (CASSCF) and complete active space second order perturbation (CASPT2) levels of theory. The effect of water on the lowest-energy path through the ethylenic conical intersection is a lowering of the energy barrier. This is explained by stabilization of the excited state, which has zwitterionic character in the vicinity of the conical intersection due to its similarity with the conical intersection of ethylene. In contrast to this, the path that involves the (n_N, π^*) state is destabilized by hydrogen bonding, although the bulk solvent effect reduces the destabilization. Overall, this path should remain energetically accessible.

Keywords: Cytosine; Photophysics; Computations; Solvation; Conical intersections

1. Introduction

The photophysics of the DNA nucleobases has been intensively studied in the last decade [1–9]. One of the most characteristic traits is a very short excited-state lifetime for all bases, and calculations have provided information about the mechanisms behind the fast radiationless decay of the bases [10–28]. However, while most computational studies have modeled the gas-phase photophysics, experiments on the nucleobase monomers have been carried out under different conditions. In addition to the gas-phase experiments on isolated bases [3,7,8], measurements have been carried out on gas-phase clusters of a base with one or more water molecules, or clusters of two bases [29–33], and in nucleosides and nucleotides in solution [1,2,4,5,9]. The purpose of this paper is to approach some of these experiments by modeling the effect of water on the excited-state decay of singlet excited cytosine. Water is considered here explicitly in calculations of clusters of cytosine with a single water molecule, and as a bulk solvent using the polarizable continuum model (PCM), where the molecule is embedded in a cavity that models the solvent [34,35]. The approach is similar to the one used recently for a study of solvent effects on the photophysics of uracil, thymine and some of their derivatives [22,25], although here the complete active space self-consistent field (CASSCF) and complete active space second order perturbation (CASPT2) methodologies are used for the excited-state calculations, instead of time-dependent (TD) density functional theory (DFT).

Most measurements of the excited-state lifetime of cytosine lie below 10 ps, although the exact value depends on the experimental conditions. Thus, the lifetime in the gas phase was first determined to be 3.2 ps [3]. However, more than one decay component has been detected in more recent experiments with higher resolution. Thus, the decay has been described with three components (one of less than 50 fs, one of 820 fs, and one of 3.2 ps) [7], while other authors describe a decay with two components of 0.16 and 1.9 ps [8]. In addition to that, a long living dark state of approximately 300 ns has been detected in the gas phase with a photoionization technique [36]. In water, transient absorption [1,5] and fluorescence up-conversion [2] experiments for cytosine, its nucleoside and its nucleotide gave a lifetime between 700 fs and 1.0 ps, while later on values of 400–530 fs were reported [4]. A biexponential fitting with one component of approximately 200 fs and another one of approximately 1 ps was also discussed for fluorescence experiments [4]. More recent transient absorption experiments have been described as a biexponential decay with a short component of up to 3 ps, approximately, and a longer one of 10–30 ps [9]. Turning to the computational results, calculations have established that the most favorable decay path for cytosine and cytidine,

* Corresponding author. Tel.: +34 972418362; fax: +34 972418356.
E-mail address: lluis.blancafort@udg.es (L. Blancafort).

1010-6030/$ – see front matter © 2007 Elsevier B.V. All rights reserved.
doi:10.1016/j.jphotochem.2007.04.015

in the gas phase, involves passage through a conical intersection of the ethylenic type, which is separated by a small barrier from the minimum of the spectroscopically active (π, π^*) state [18,20,28]. In a recent paper by one of us, the barrier was estimated as approximately 0.1 eV [37]. Other authors have suggested the existence of a barrierless channel from the Franck-Condon structure to the conical intersection, but this could not be confirmed [23]. Moreover, in the gas phase there is an additional, energetically accessible path that involves the (n_N, π^*) state (excitation from the nitrogen lone pair) [37]. The path leads from the (π, π^*) minimum to a minimum of the (n_N, π^*) state, and from there to a near-lying conical intersection with the ground state. The estimated barrier for this path was 0.2 eV, and the minima of the (π, π^*) and (n_N, π^*) states are isoenergetic. A third path involving the (n_O, π^*) state goes through a minimum of that state that is slightly higher in energy than the (π, π^*) minimum (approximately 0.1 eV), and leads to a higher-lying conical intersection (>1.0 eV) [37].

The effect of water on the two energetically favored paths, the one to the ethylenic type conical intersection and the one through the (n_N, π^*) state, has been studied here using the CASPT2//CASSCF methodology. The (n_O, π^*) path has not been considered as it lies substantially higher in energy in the gas phase, and it can be expected that the overall solvent effect will destabilize the (n_O, π^*) state. Critical points (excited-state minima and conical intersections) and minimum energy paths (intrinsic reaction coordinates) are calculated at the CASSCF level, and the gas-phase energetics are recalculated with single-point CASPT2 calculations on the CASSCF structures. For the ethylenic path, a valence-bond based characterization of the degenerate states at the conical intersection indicates that one of the states has zwitterionic character [37]. Thus, it can be expected that this path will be stabilized in water, and the present calculations confirm this hypothesis. In contrast to this, simple qualitative arguments indicate that the (n_N, π^*) state will be less accessible in water because of its destabilization by hydrogen bonding. The question then is if the (n_N, π^*) path is blocked in water or not, and the calculations suggest that it is destabilized but remains energetically accessible.

2. Computational details

The calculations were carried out at the CASSCF and CASPT2 levels of theory, using the 6-31+G* basis set for consistency with the previous gas-phase study [37]. Excited-state optimizations and minimum energy path calculations in the gas phase and in solvent are carried out at the CASSCF level using Gaussian03 [38], while the CASPT2 gas-phase energies are calculated with Molcas5.4 [39] (real level shift [40] parameter of 0.2 a.u.). The bulk solvent effect is taken into account in the CASSCF calculations using the self-consistent reaction field (SCRF) methodology and the conductor version of the polarizable continuous model (CPCM) implemented in Gaussian03 [41]. These calculations are referred to as CPCM–CASSCF. The density matrix used for the SCRF part in the CPCM–CASSCF optimizations and IRC calculations is the CASSCF state-averaged one. This is not the standard procedure, as ideally the density matrix of the root of interest (the second root here) should be used; however, the use of a state-specific root leads to convergence problems in the vicinity of conical intersections, presumably because of root flipping. To avoid these problems, the state-averaged density was used. A state-specific density matrix should also be used in CPCM–CASPT2 calculations, and therefore the solvent effect has not been calculated at the CASPT2 level. Conical intersections are not optimized at the CPCM–CASSCF level.

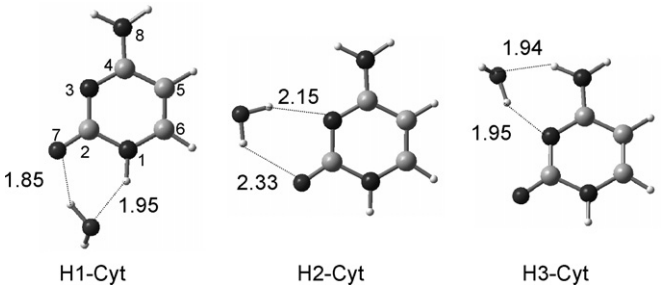

Fig. 1. B3LYP/6-311G** optimized structures of cytosine monohydrates (distances in Å).

2.1. Vertical excitations

The vertical excitations for isolated cytosine and the three monohydrates shown in Fig. 1 are calculated on geometries obtained at the B3LYP/6-311G** level of theory (see Table 1). The excitations are calculated in the gas phase at the CASSCF and CASPT2 levels, and in solution at the CPCM–CASSCF level (non-equilibrium [41] version). The CASPT2 energies in solution are approximated by adding the difference between the CASSCF gas phase and CPCM values to the CASPT2 gas phase value. Besides, the energies are obtained in two series of calculations, one with a (12,11) active space that yields the energy of the lowest-lying (π, π^*) and (n_N, π^*) states, and one with a (12,12) active space that yields the energy of the lowest-lying (π, π^*) and (n_O, π^*) states (see reference [37] for a description of the active space orbitals). For this reason, two values are reported in Table 1 for the energy of the (π, π^*) state for gas phase cytosine (Cyt) and H2-Cyt (see Fig. 1 for the labeling). The averages of the values in Table 1 for the three monohydrates are the estimated vertical excitations in water listed in Table 2.

2.2. CASSCF optimizations and minimum energy paths

The optimizations and minimum energy path calculations (intrinsic reaction coordinate, IRC [42]) were carried out with (10,9) and (12,11) active spaces for the path to the ethylenic type intersection and for the (n_N, π^*) path, respectively. The minimum-energy paths between the minima of the spectroscopic sate, $(\pi, \pi^*)_{Min}$, and the ethylenic type intersection $(Eth)_X$ or the minimum of the (n_N, π^*) state, $(n_N, \pi^*)_{Min}$, are the IRC from the corresponding optimized transition structures. The details of these calculations can be found in reference [37]. The CASSCF transition structures correspond to displacement 0.0 a.u. along

Table 1
CASSCF and CASPT2 photophysical energies (vertical excitations, except where indicated) of lowest singlet states for cytosine and cytosine monohydrates

Structure	State	E_{CASSCF} [eV]	E_{CASPT2} [eV]	E^{CPCM}_{CASSCF} [eV]	ΔE^{CPCM}_{CASSCF} [a] [eV]	$E_{CASPT2} + \Delta E^{CPCM}_{CASSCF}$ [eV]
Cyt	(π, π^*)[b]	5.17	4.34	5.26	0.09	4.43
	(π, π^*)[c]	5.26	4.27	5.46	0.20	4.47
	(n_N, π^*)[c]	5.87	5.20	6.32	0.45	5.65
	(n_O, π^*)[b]	6.00	5.51	6.70	0.70	6.21
	$(\pi, \pi^*)_{0-0}$[b]	4.18	3.75	–	–	–
H1-Cyt	(π, π^*)[b]	5.15	4.39	5.26	0.11	4.50
	(n_O, π^*)[b]	6.27	5.76	6.83	0.56	6.32
	$(\pi, \pi^*)_{0-0}$[b]	4.17	4.08	–	–	–
H2-Cyt	(π, π^*)[b]	5.19	4.39	5.28	0.09	4.48
	(π, π^*)[c]	5.02	4.35	5.28	0.26	4.61
	(n_N, π^*)[c]	5.96	5.45	6.32	0.36	5.81
	(n_O, π^*)[b]	6.17	5.68	6.75	0.58	6.26
H3-Cyt	(π, π^*)[c]	5.29	4.33	5.48	0.19	4.52
	(n_N, π^*)[c]	6.22	5.52	6.49	0.27	5.79
	$(\pi, \pi^*)_{0-0}$[c]	4.10	3.91	–	–	–

[a] Difference between CASSCF gas-phase and CPCM energies.
[b] (12,12) Active space.
[c] (12,11) Active space.

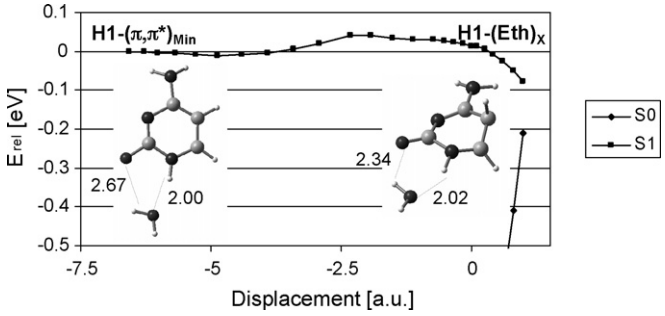

Fig. 2. CASPT2//CASSCF energy profile for decay along ethylenic path of H1-Cyt (distances in Å).

the *x*-axis of the energy profiles of Figs. 2, 3 and 5. Similarly to what happened for isolated cytosine, the point of highest energy along the IRC of the ethylenic path is displaced with respect to the CASSCF transition structure. In all cases, the barriers are given as the energy difference between the minimum of the spectroscopic state, $(\pi, \pi^*)_{Min}$, and the point of highest energy along the reaction coordinate. Structure H3-$(n_N, \pi^*)_X$ could not be fully optimized because the water molecule is only weakly bound to the cytosine nitrogen atom, and this caused difficulties

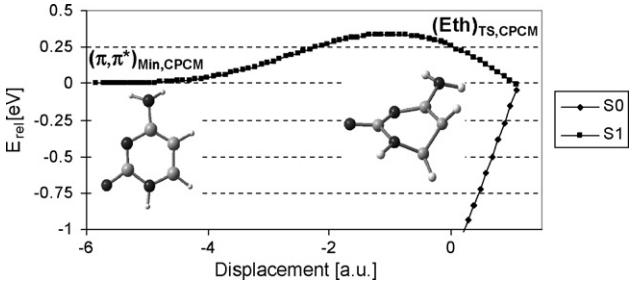

Fig. 3. CPCM–CASSCF energy profile for decay along ethylenic path of cytosine in water.

Table 2
Estimated vertical excitations for cytosine in water

State	E_{avg} [a] [eV]	ΔE [b] [eV]
(π, π^*)	4.53 ± 0.04	+0.2
(n_N, π^*)	5.80 ± 0.01	+0.6
(n_O, π^*)	6.29 ± 0.03	+0.8

[a] Average of $E_{CASPT2} + \Delta E^{CPCM}_{CASSCF}$ for cytosine monohydrates (see Table 1).
[b] Difference with respect to gas phase excitations.

in the optimization, but a point of degeneracy was located using only the energy difference component of the conical intersection gradient for the optimization [43].

3. Results and discussion

3.1. Ground-state structures and vertical excitations

The effect of water on the vertical excitations is considered first by including explicitly one water molecule in the calculation. The vertical excitations are computed for the three doubly hydrogen-bonded isomers shown in Fig. 1. Previous studies indicate that H1-Cyt and H3-Cyt are the most stable isomers [44,45], while the stability of H2-Cyt depends on the level of calculation. Here, the structures have been optimized at the B3LYP/6-311G** level of theory, and H1-Cyt is the most stable isomer, with H2-Cyt and H3-Cyt lying 5.7 and 0.6 kcal mol^{-1} above, respectively. The lower stability of H2-Cyt is explained by the fact that it has weaker hydrogen bonds, as seen on the longer hydrogen bonds.

The vertical excitations for isolated cytosine and its monohydrates (gas phase) are listed in Table 1. For comparison with the monohydrates, the vertical excitation of isolated cytosine is also calculated on the B3LYP/6-311G** optimized ground-state geometry. At that geometry, the gas phase vertical excitation

of the (π, π^*) state, which is approximately 4.3 eV, differs from the value of approximately 4.5 eV obtained using the CASSCF(8,7)/6-31G* optimized geometry [37], and it underestimates the experimental absorption maximum of 4.65 eV. Coordination of a water molecule to the O_8 and/or N_3 atoms raises the energy of the (π, π^*) CASPT2 vertical transition by approximately 0.1 eV (compare the values for isolated and hydrated cytosine in Table 1). Inclusion of the bulk solvation effect also raises the vertical excitation of the (π, π^*) state by approximately 0.1 eV (sixth column of Table 1). Overall, the estimated value of approximately 4.5 eV for the vertical (π, π^*) excitation in solution is in good agreement with the maximal absorption of 271 nm (4.57 eV) measured for the nucleoside and nucleotide of cytosine in water [4]. However, this corresponds to a blue shift of approximately 0.2 eV with respect to isolated cytosine, while experimentally a small red shift of less than 0.1 eV is observed [4,46]. The failure to reproduce the experimental red shift may be due to not including the solvent effect in the CASPT2 calculation, but it may also be caused by other limitations of the present approach. For instance, the (π, π^*) excitation is very sensitive to the level of theory used to obtain the ground-state geometry, and a more accurate determination of the ground-state geometries in the gas phase and in solution may also be important to get the correct solvent shift.

The effect of water coordination on the vertical excitations of the (n, π^*) states is approximately 0.3 eV. Similar values have been reported for the scaled CIS/6-311G** (configuration interaction with singles) vertical excitations of cytosine trihydrate [47]. The calculated (n_N, π^*) and (n_O, π^*) vertical transitions in solution are 5.8 and 6.3 eV, respectively. The estimated blue shift of the (n_O, π^*) state in water, of about 0.8 eV, is larger than the values of 0.4–0.5 eV calculated for uracil and thymine with PCM-TDDFT [22].

Turning to the gas-phase 0–0 transitions of the monohydrates, the calculated 0–0 transitions for H1-Cyt and H3-Cyt are 4.08 and 3.91 eV, respectively (see Table 1). This indicates an increase of 0.2–0.3 eV with respect to isolated cytosine, which has a calculated 0–0 transition of 3.75 eV. For H1-Cyt, the increase in the 0–0 energy is an effect of the reduced hydrogen-bonding capacity of the spectroscopically active (π, π^*) state, which results in its destabilization compared to the ground state. Thus, the hydrogen bond between the water molecule and the carbonyl oxygen is considerably weakened at the minimum of this state, H1-(π, π^*)$_{Min}$, with respect to the ground-state minimum. This can be seen in the increase of the bond length from approximately 2 Å to 2.7 Å (see bond lengths in Figs. 1 and 2).

3.2. Decay paths

The ethylenic and (n_N, π^*) decay paths in solution have been recomputed reoptimizing the stationary points and minimum energy paths with the CPCM approach. In addition to that, the two paths have been optimized for the H1-Cyt and H3-Cyt monohydrates, respectively. These optimizations have been carried out in the gas phase because test calculations with the CPCM approach on H1-Cyt showed that the optimization of the excited-state minimum leads to breaking of the hydrogen bond between the water molecule and the carbonyl oxygen.

The *ethylenic path* connects the minimum of the spectroscopic (π, π^*) state, (π, π^*)$_{Min}$, with the conical intersection of ethylenic type, (Eth)$_X$. This path has been optimized for the H1-Cyt monohydrate, where the water molecule is hydrogen bonded to the carbonyl oxygen. The optimized excited-state structure H1-(π, π^*)$_{Min}$ has an inverted bond pattern with respect to the ground state, as described previously for (π, π^*)$_{Min}$ of isolated cytosine (elongation of the O_7–C_2, N_3–C_4, and C_5–C_6 bonds, and shortening of the C_2–N_3 and C_4–C_5 bonds). At the same time, the hydrogen bond to O_7 is significantly stretched to 2.67 Å, from a ground-state value of approximately 2 Å (1.85 Å at the B3LYP/6-311G** level and 2.04 Å at the CASSCF level). The optimized conical intersection structure H1-(Eth)$_X$ is shown in Fig. 2. The structure is similar to its analogue for isolated cytosine, and both structures have a H–C_5–C_6–H dihedral angle of 118° [37]. The effect of hydration is therefore comparable to what happens with uracil tetrahydrate [22], where the structure of the ethylenic S_1/S_0 conical intersection is similar to the gas-phase one. The behavior of the hydrogen bond between the water molecule and the carbonyl oxygen, which is considerably weakened at H1-(π, π^*)$_{Min}$ (H–O bond length of 2.67 Å) and partially recovered at H1-(Eth)$_X$ (2.34 Å), is related with the changes in the π electron density at the cytosine oxygen in the excitation. This magnitude is measured using the diagonal elements of the one-electron density matrix of the active space orbitals after localization (see the valence-bond based analyses in references [12,37]). Thus, the π electron density on S_1 at the FC minimum of isolated cytosine is 1.41 a.u.; the value is reduced to 1.08 a.u. at (π, π^*)$_{Min}$ and recovered to 1.44 a.u. at (Eth)$_X$. An elongation of the H–O bond in the (π, π^*) state has been also found experimentally and theoretically for a 2-pyridone-water cluster analogous to H1-Cyt, although there the elongation is more substantial (more than 2 Å) [48].

The ethylenic decay path, calculated at the CASPT2//CASSCF level for H1-Cyt, is shown in Fig. 2. The barrier for the decay is 0.05 eV, which is somewhat lower than the value of 0.11 eV calculated in the gas phase. The difference can be explained on the basis of the reduced hydrogen-bonding capacity of the carbonyl oxygen in the (π, π^*) state discussed above. The hydrogen bond at H1-(π, π^*)$_{Min}$ is weaker than at H1-(Eth)$_X$, i.e. (Eth)$_X$ is more stabilized by hydrogen bond formation than (π, π^*)$_{Min}$, and this explains the lowering of the barrier upon hydration.

The CPCM–optimized structures, (π, π^*)$_{Min,CPCM}$ and (Eth)$_{TS,CPCM}$, have similar structures to their analogues in isolated and monohydrated cytosine. The corresponding decay path, calculated at the CPCM–CASSCF level, is shown in Fig. 3. At the last optimized structure along the path, in the direction that increases the torsion, the energy gap between the ground and excited states is less than 0.05 eV, which points to the existence of the S_1/S_0 conical intersection at the CPCM–CASSCF level. The CPCM–CASSCF barrier to access the intersection is 0.33 eV, which is lower than the CASSCF gas-phase barrier of 0.51 eV. While the CPCM–CASPT2 values are not available, on the basis of the CASSCF values it appears that inclusion of the bulk water

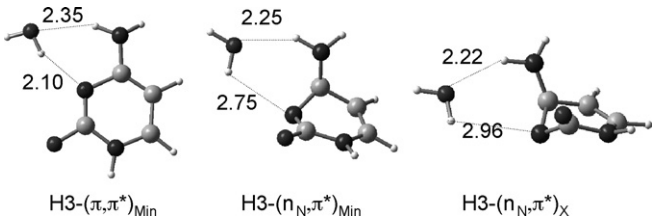

Fig. 4. CASSCF optimized structures for (n_N, π^*) decay path of H3-Cyt (distances in Å).

solvent also lowers the barrier for the decay through the ethylenic type intersection. This result can be explained on the basis of the zwitterionic nature of the excited state, shown in a previous valence-bond analysis [37]. Thus, $(Eth)_X$ is an analogue of the conical intersection of ethylene, where the excited-state wave function has zwitterionic character, and the charge separation is favored by the solvation.

The (n_N, π^*) *path* has been studied for H3-Cyt, where the water molecule is hydrogen bonded to the nitrogen atom that carries the lone pair involved in the excitation. In the gas phase, this path connects (π, π^*)$_{Min}$ with a minimum of the (n_N, π^*) state, (n_N, π^*)$_{Min}$. Next to (n_N, π^*)$_{Min}$ there is a conical intersection with the ground state, (n_N, π^*)$_X$ [37]. The corresponding structures H3-(π, π^*)$_{Min}$, H3-(n_N, π^*)$_{Min}$ and H3-(n_N, π^*)$_X$ have been located for the monohydrate (see Fig. 4). The optimized H3-(π, π^*)$_{Min}$ structure is similar to the minimum of the (π, π^*) state obtained for H1-Cyt, although the hydrogen bond with the N_2 atom of cytosine keeps its ground-state bond length of approximately 2 Å. In contrast to this, the hydrogen bond is substantially stretched at H3-(n_N, π^*)$_{Min}$ (2.75 Å) and H3-(n_N, π^*)$_X$ (2.96 Å). H3-(n_N, π^*)$_X$ is geometrically similar to the unhydrated structure (n_N, π^*)$_X$. Both structures are characterized by an out-of-plane bending of the N_3 ring atom and the amino substituent, due to an electronic repulsion caused by the excitation [12]. Thus, the N_3–C_4–C_5–C_6 dihedral angle is −27° for H3-(n_N, π^*)$_X$ and −26° for (n_N, π^*)$_X$, while the N_8–C_4–C_5–C_6 dihedral is 107° and 106° for the hydrated and unhydrated species, respectively.

The CASPT2//CASSCF energies of the H3-(n_N, π^*)$_{Min}$ and H3-(n_N, π^*)$_X$ critical points relative to H3-(π, π^*)$_{Min}$ are 0.27 and 0.36 eV, respectively. The last value is an average of the relative CASPT2 energies of the two states at the CASSCF optimized conical intersection, which are 0.17 eV and 0.56 eV (CASPT2 energy gap of 0.39 eV). These values show that the (n_N, π^*) path is destabilized by the presence of the water molecule, as the (n_N, π^*)$_{Min}$ and (π, π^*)$_{Min}$ structures of isolated cytosine are isoenergetic. The destabilization of the (n_N, π^*) state is in agreement with chemical intuition. Optimization of the transition structure connecting H3-(π, π^*)$_{Min}$ and H3-(n_N, π^*)$_{Min}$ would allow for an estimate of the barrier along that path, but that structure could not be located in the present work. Attempts to optimize the transition structure lead to a transition structure between different isomers of (n_N, π^*)$_{Min}$ with the water molecule coordinated to the amino group or the carbonyl oxygen. This suggests that a full optimization of the reaction path that connects (π, π^*)$_{Min}$ with (n_N, π^*)$_{Min}$ in water requires the inclusion of more water molecules.

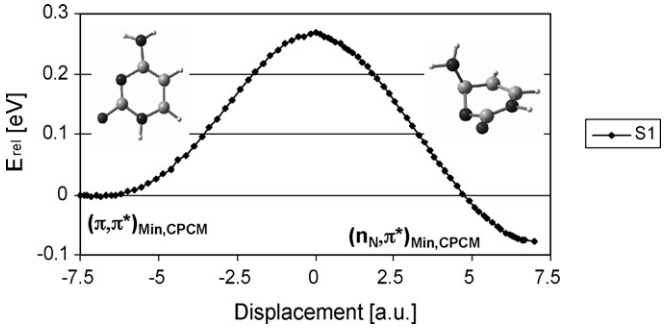

Fig. 5. CPCM–CASSCF energy profile along (n_N, π^*) path for cytosine in solution.

The bulk solvent effect on the (n_N, π^*) path was estimated optimizing structures (n_N, π^*)$_{Min,CPCM}$ and (n_N, π^*)$_{TS,CPCM}$, and calculating the minimum energy path from (π, π^*)$_{Min,CPCM}$ to (n_N, π^*)$_{Min,CPCM}$ (see Fig. 5). The conical intersection between the ground and (n_N, π^*) states was not located at the CPCM–CASSCF level of theory; however, the S_1/S_0 energy gap at (n_N, π^*)$_{Min,CPCM}$, of 0.4 eV, is small enough that the occurrence of a near-lying conical intersection can be expected, in analogy to the gas phase. Furthermore, the CASSCF barrier along the path to (n_N, π^*)$_{Min,CPCM}$ is 0.27 eV, which is lower than the value of 0.46 eV calculated for cytosine in the gas phase. Thus, the bulk solvent effect appears to stabilize the (n_N, π^*) path by a similar amount than the destabilization by hydrogen bonding. The stabilization might be due to an increase in the dipole moment, from 7.0 Debye at (π, π^*)$_{Min,CPCM}$ to 7.4 Debye at (n_N, π^*)$_{Min,CPCM}$. However, hydration of cytosine by water molecules will probably change these values, and inclusion of a hydration shell will be necessary for a better estimate of the bulk solvent effect on the path.

4. Conclusions

The solvation effects on the photophysics of cytosine are considered here from two points of view: hydration of the base by hydrogen bonding to its heteroatoms, and a bulk solvation effect, mainly of electrostatic origin. The calculations on the monohydrates are relevant for the gas-phase spectroscopy of these complexes. For the experiments in water, both hydration and bulk solvation effects are important. These effects are considered separately, but the present results can be used as qualitative estimates of the total solvation effect on the decay paths. Moreover, the bulk solvent effect is only calculated at the CASSCF level here, by comparing the CPCM–CASSCF results with the gas-phase CASSCF ones. Although it would be desirable to calculate the solvent effect at the CASPT2 level, we are implicitly relying on the fact that the CASPT2 correction (dynamic correlation) is little affected by the bulk solvent. However, the opposite cannot be excluded, and therefore the conclusions about the solvent effect remain to be confirmed at an improved level of theory.

The molecular solvation effects on the two paths are summarized in Table 3 ($\Delta(\Delta E)_{H_2O}$). The energetically more favorable ethylenic pathway is stabilized by hydration. In contrast to this, and in agreement with qualitative arguments, the (n_N, π^*) path-

Table 3
Energy barriers for cytosine excited state decay paths (gas phase values and water effects)

Path	ΔE_{gas}[a] [eV]	$\Delta(\Delta E)_{H_2O}$[b] [eV]	$\Delta(\Delta E)_{CPCM}$[c] [eV]
(Eth)	0.11	−0.05	−0.05
(n_N, π^*)	0.21	∼+0.3	−0.19

[a] CASPT2//CASSCF gas-phase barriers (values from reference [37]).
[b] Difference between CASPT2//CASSCF gas-phase barriers for cytosine monohydrates and cytosine.
[c] Difference between CPCM–CASSCF and CASSCF gas-phase barriers.

way is destabilized by a sizeable amount (approximately 0.3 eV) by hydration at the N_3 ring nitrogen. The energies of H3-(n_N, π^*)$_{Min}$ and H3-(n_N, π^*)$_X$ relative to the FC ground state energy are 4.18 and 4.27 eV, while the vertical excitation energy in the gas phase, for H3-Cyt, is 4.33 eV. This suggests that, for H3-Cyt, the (n_N, π^*) path remains accessible after vertical excitation, although the ethylenic pathway is even more favored than in the gas phase.

Turning to the photophysics in water, both molecular and bulk effects lower the barrier associated to the ethylenic decay path. This would suggest a shortening of the excited-state lifetime of cytosine in water with respect to the gas phase. However a comparison of the lifetimes is problematic because, in addition to the energies along the path, the lifetime depends on several other factors, such as the excitation energy and the viscosity effect of the solvent. The calculations also indicate that bulk solvation might compensate the energy increase for the structures that correspond to the (n_N, π^*) path, although this effect is probably overestimated by the present CPCM calculations, that are carried out on bare cytosine. However the results suggest that the (n_N, π^*) path remains energetically accessible in water, with respect to the vertical excitation. In fact, it has recently been suggested that an (n, π^*) state is responsible for the appearance of a second component (10–30 ps) in the photophysics of cytidine in water [9]. This component could be explained with the help of the (n_N, π^*) path shown here. However, to confirm this hypothesis more accurate calculations are necessary, including the full characterization of the (n_N, π^*) path in water, using a larger hydration shell, and a better determination of the energy difference between (n_N, π^*)$_{Min}$ and the adjacent (n_N, π^*)$_X$ conical intersection.

Acknowledgments

This work has been supported by the Ramón y Cajal program from the Spanish Ministerio de Educación y Ciencia (MEC), grant CTQ2005-04563 from the Dirección General de Investigación (MEC), a grant from the Francesca Roviralta Foundation, and a research grant from the Universitat de Girona (Ref. 7E200402).

References

[1] J.M.L. Pecourt, J. Peon, B. Kohler, J. Am. Chem. Soc. 123 (2001) 10370–10378.
[2] J. Peon, A.H. Zewail, Chem. Phys. Lett. 348 (2001) 255–262.
[3] H. Kang, K.T. Lee, B. Jung, Y.J. Ko, S.K. Kim, J. Am. Chem. Soc. 124 (2002) 12958–12959.
[4] D. Onidas, D. Markovitsi, S. Marguet, A. Sharonov, T. Gustavsson, J. Phys. Chem. B 106 (2002) 11367–11374.
[5] R.J. Malone, A.M. Miller, B. Kohler, Photochem. Photobiol. 77 (2003) 158–164.
[6] C.E. Crespo-Hernández, B. Cohen, P.M. Hare, B. Kohler, Chem. Rev. 104 (2004) 1977–2202.
[7] S. Ullrich, T. Schultz, M.Z. Zgierski, A. Stolow, Phys. Chem. Chem. Phys. 6 (2004) 2796–2801.
[8] C. Canuel, M. Mons, F. Piuzzi, B. Tardivel, I. Dimicoli, M. Elhanine, J. Chem. Phys. 122 (2005) 074316.
[9] P.M. Hare, C.E. Crespo-Hernandez, B. Kohler, Proc. Natl. Acad. Sci. U.S.A. 104 (2007) 435–440.
[10] B. Mennucci, A. Toniolo, J. Tomasi, J. Phys. Chem. A 105 (2001) 7126–7134.
[11] B. Mennucci, A. Toniolo, J. Tomasi, J. Phys. Chem. A 105 (2001) 4749–4757.
[12] N. Ismail, L. Blancafort, M. Olivucci, B. Kohler, M.A. Robb, J. Am. Chem. Soc. 124 (2002) 6818–6819.
[13] M. Merchán, L. Serrano-Andrés, J. Am. Chem. Soc. 125 (2003) 8108–8109.
[14] L. Blancafort, M.A. Robb, J. Phys. Chem. A 108 (2004) 10609–10614.
[15] S. Matsika, J. Phys. Chem. A 108 (2004) 7584–7590.
[16] H. Chen, S.H. Li, J. Phys. Chem. A 109 (2005) 8443–8446.
[17] L. Serrano-Andrés, M. Merchán, R. Lindh, J. Chem. Phys. 122 (2005) 104107.
[18] K. Tomic, J. Tatchen, C.M. Marian, J. Phys. Chem. A 109 (2005) 8410–8418.
[19] M.Z. Zgierski, S. Patchkovskii, T. Fujiwara, E.C. Lim, J. Phys. Chem. A 109 (2005) 9384–9387.
[20] M.Z. Zgierski, S. Patchkovskii, E.C. Lim, J. Chem. Phys. 123 (2005) 081101.
[21] H. Chen, S.H. Li, J. Chem. Phys. 124 (2006) 154315.
[22] T. Gustavsson, A. Banyasz, E. Lazzarotto, D. Markovitsi, G. Scalmani, M.J. Frisch, V. Barone, R. Improta, J. Am. Chem. Soc. 128 (2006) 607–619.
[23] M. Merchan, R. Gonzalez-Luque, T. Climent, L. Serrano-Andres, E. Rodriguez, M. Reguero, D. Pelaez, J. Phys. Chem. B 110 (2006) 26471–26476.
[24] S. Perun, A.L. Sobolewski, W. Domcke, J. Phys. Chem. A 110 (2006) 13238–13244.
[25] F. Santoro, V. Barone, T. Gustavsson, R. Improta, J. Am. Chem. Soc. 128 (2006) 16312–16322.
[26] L. Serrano-Andres, M. Merchan, A.C. Borin, Chem. Eur. J. 12 (2006) 6559–6571.
[27] L. Serrano-Andres, M. Merchan, A.C. Borin, Proc. Natl. Acad. Sci. U.S.A. 103 (2006) 8691–8696.
[28] M.Z. Zgierski, S. Alavi, Chem. Phys. Lett. 426 (2006) 398–404.
[29] E. Nir, K. Kleinermanns, M.S. de Vries, Nature 408 (2000) 949–951.
[30] I. Hunig, C. Plutzer, K.A. Seefeld, D. Lowenich, M. Nispel, K. Kleinermanns, Chemphyschem 5 (2004) 1427–1431.
[31] H.H. Ritze, H. Lippert, E. Samoylova, V.R. Smith, I.V. Hertel, W. Radloff, T. Schultz, J. Chem. Phys. 122 (2005).
[32] E. Samoylova, H. Lippert, S. Ullrich, I.V. Hertel, W. Radloff, T. Schultz, J. Am. Chem. Soc. 127 (2005) 1782–1786.
[33] C. Canuel, M. Elhanine, M. Mons, F. Piuzzi, B. Tardivel, I. Dimicoli, Phys. Chem. Chem. Phys. 8 (2006) 3978–3987.
[34] M. Cossi, V. Barone, M.A. Robb, J. Chem. Phys. 111 (1999) 5295–5302.
[35] J. Tomasi, B. Mennucci, R. Cammi, Chem. Rev. 105 (2005) 2999–3093.
[36] E. Nir, M. Muller, L.I. Grace, M.S. de Vries, Chem. Phys. Lett. 355 (2002) 59–64.
[37] L. Blancafort, Photochem. Photobiol., in press. Available on the web under: http://phot.allenpress.com/pdfserv/10.1562%2F2006-05-29-RA-903.
[38] M.J. Frisch, G.W. Trucks, H.B. Schlegel, G.E. Scuseria, M.A. Robb, J.R. Cheeseman, J.J.A. Montgomery, T. Vreven, K.N. Kudin, J.C. Burant, J.M. Millam, S.S. Iyengar, J. Tomasi, V. Barone, B. Mennucci, M. Cossi, G. Scalmani, N. Rega, G.A. Petersson, H. Nakatsuji, M. Hada, M. Ehara, K. Toyota, R. Fukuda, J. Hasegawa, M. Ishida, T. Nakajima, Y. Honda, O. Kitao, H. Nakai, M. Klene, X. Li, J.E. Knox, H.P. Hratchian, J.B. Cross, C. Adamo, J. Jaramillo, R. Gomperts, R.E. Stratmann, O. Yazyev, A.J. Austin, R.

Cammi, C. Pomelli, J.W. Ochterski, P.Y. Ayala, K. Morokuma, G.A. Voth, P. Salvador, J.J. Dannenberg, V.G. Zakrzewski, S. Dapprich, A.D. Daniels, M.C. Strain, O. Farkas, D.K. Malick, A.D. Rabuck, K. Raghavachari, J.B. Foresman, J.V. Ortiz, Q. Cui, A.G. Baboul, S. Clifford, J. Cioslowski, B.B. Stefanov, G. Liu, A. Liashenko, P. Piskorz, I. Komaromi, R.L. Martin, D.J. Fox, T. Keith, M.A. Al-Laham, C.Y. Peng, A. Nanayakkara, M. Challacombe, P.M.W. Gill, B. Johnson, W. Chen, M.W. Wong, C. González, J.A. Pople, Gaussian03 Revision B.02, Gaussian, Inc., Pittsburgh, PA, 2003.

[39] K. Andersson, M. Barysz, A. Bernhardsson, M.R.A. Blomberg, Y. Carissan, D.L. Cooper, M. Cossi, T. Fleig, M.P. Fülscher, L. Gagliardi, Cd. Graaf, B.A. Hess, G. Karlström, R. Lindh, P.-Å. Malmqvist,P. Neogrády, J. Olsen, B.O. Roos, B. Schimmelpfennig, M. Schütz, L. Seijo, L. Serrano-Andrés, P.E.M. Siegbahn, J. Stålring,T. Thorsteinsson, V. Veryazov, M. Wierzbowska, P.O. Widmark, Molcas Version 5.4, University of Lund, Sweden, 2003.

[40] B.O. Roos, K. Andersson, Chem. Phys. Lett. 245 (1995) 215–223.

[41] M. Cossi, V. Barone, J. Chem. Phys. 112 (2000) 2427–2435.

[42] C. González, H.B. Schlegel, J. Phys. Chem. 94 (1990) 5523–5527.

[43] M.J. Bearpark, M.A. Robb, H.B. Schlegel, Chem. Phys. Lett. 223 (1994) 269–274.

[44] C. Aleman, Chem. Phys. Lett. 302 (1999) 461–470.

[45] T. van Mourik, D.M. Benoit, S.L. Price, D.C. Clary, Phys. Chem. Chem. Phys. 2 (2000) 1281–1290.

[46] R. Abouaf, J. Pommier, H. Dunet, P. Quan, P.C. Nam, M.T. Nguyen, J. Chem. Phys. 121 (2004) 11668–11674.

[47] M.K. Shukla, J. Leszczynski, J. Phys. Chem. A 106 (2002) 11338–11346.

[48] R. Brause, M. Schmitt, K. Kleinermanns, J. Phys. Chem. A 111 (2007) 3287–3293.